Continuous Observations of Chlorophyll Fluorescence and Related Parameters in Massachusetts Bay 2005 – 2019

Massachusetts Water Resources Authority
Environmental Quality Department
Report 2020-09

Continuous observations of chlorophyll fluorescence and related parameters in Massachusetts Bay, 2005 - 2019

Principal Investigator:	Dr. Collin Roesler
Institution:	Bowdoin College Department of Earth and Oceanographic Science
Address:	6800 College Station Brunswick, ME 04011
Phone:	207-725-3842
Email:	croesler@bowdoin.edu

Period of Performance: 1 July 2019 - 30 June 2020

Citation:

Roesler CS. 2020. Continuous observations of chlorophyll fluorescence and related parameters in Massachusetts Bay, 2005 – 2019. Boston: Massachusetts Water Resources Authority. Report 2020-09. 27 p.

Environmental Quality Department reports can be downloaded from
http://www.mwra.com/harbor/enquad/trlist.html

Cover. Sue Drapeau on research vessel (photo credit Collin Roesler). Inset: Buoy A01 (photo credit Bob Fleming).

SUMMARY

Since late 2000, the Massachusetts Water Resources Authority (MWRA) has discharged treated wastewater from its Deer Island Treatment Plant in Boston into Massachusetts Bay through an outfall 9.5 miles (15 km) offshore. To help ensure that nutrients in the discharge do not contribute to eutrophication, an excess growth of marine algae, or phytoplankton, the MWRA monitoring program surveys bay phytoplankton conditions from a research vessel about once a month. Chlorophyll is the indicator of phytoplankton, measured during surveys. The results demonstrate that bay chlorophyll has remained at healthy levels, including near the outfall.

To augment its monitoring, in particular how frequently chlorophyll is measured, since 2005 MWRA has contracted with Bowdoin College researchers to operate sensors on a buoy moored off Cape Ann in northeastern Massachusetts Bay. The sensors make continuous measurements of chlorophyll and turbidity, or water cloudiness due to suspended particles, and report hourly results in real time online (www.neracoos.org). University of Maine maintains the buoy, which collects additional observations, with support from the Northeast Regional Association of Coastal Ocean Observing Systems and MWRA.

The sensor used to detect chlorophyll is a fluorometer, which measures the red light emitted (fluoresced) by phytoplankton in response to a blue light flash. In 2016, Bowdoin added a second fluorometer, which measures red fluorescence in response to light flashes at three wavelengths to help identify multiple types of phytoplankton, and an irradiance sensor measuring above-water solar conditions to help improve quality of the fluorescence measurements. Bowdoin configures and calibrates the sensors, works with University of Maine to deploy and recover them at sea, arranges manufacturer repair and maintenance, and interprets results in the context of oceanographic conditions.

Based on all years of results, the seasonal cycle in chlorophyll includes blooms in spring and fall. In general, the overall increase in the spring bloom has 1 to 4 peaks superposed, while the fall bloom has a single lower concentration peak and a longer duration. Turbidity, influenced mainly by storms, has higher values from late winter through spring than the rest of the year, and an early fall peak; the variability is larger than for chlorophyll and the events are short and intense. **Conditions during 2018-2019 were typical of other years and did not indicate unusual water quality.**

Results also suggest the spring bloom is occurring earlier and lasting longer, and the fall bloom is also lasting slightly longer with a decreasing peak height. These variations are most likely regional and due to fluctuating temperature and salinity stratification.

Annual medians of chlorophyll at Cape Ann buoy, 2005-2019

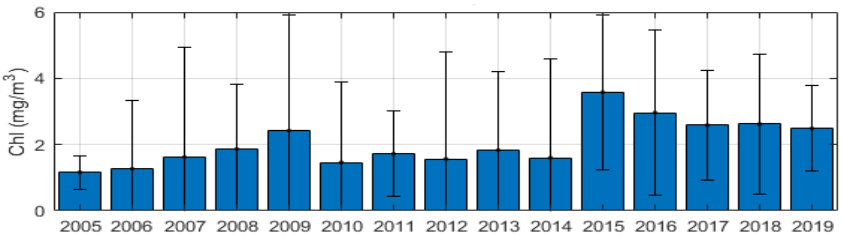

Bowdoin chlorophyll, 2005-2019: annual median (bars), standard deviation (error bars).

Chlorophyll measurements show long-term variability including modest increases during 2006-2009, relatively constant intermediate levels from 2010-2014, and higher but declining levels from 2015-2019.

A range of quality assurance methods have been improved and implemented: a new correction for drift of times measured by the irradiance sensor; corrections for calibration drift; removal of biofouled values and outliers; and a method (recently published) to correct for daytime bias of chlorophyll by non-photochemical quenching, which can cause measurements that are up to 50% lower than actual.

To help characterize phytoplankton community composition, which is the relative proportions of different phytoplankton types, the ratios of fluorescence at different wavelengths from the three-wavelength fluorometer are analyzed. This newer optical method suggests there is a seasonal pattern in the most abundant types of phytoplankton that is similar each year and consistent with results from other methods.

Introduction

This report describes work and results from 2018-2019 deployments of MWRA's continuous biological monitoring in Massachusetts Bay, performed by Bowdoin College researchers. The program focus is real-time monitoring of water quality conditions, with emphasis on marine algae (phytoplankton) through chlorophyll measurements, to improve MWRA's ability to detect changes and respond if necessary. MWRA's Ambient Monitoring Plan, attached to its National Pollutant Discharge Elimination System permit to release treated effluent from the Deer Island Wastewater Treatment Plant into Massachusetts Bay, requires this monitoring.

The program consists of bio-optical observations made at a depth of 3 m on the moored buoy off Cape Ann (Figure 1), referred to as Buoy A01 or Mooring A01, operated by University of Maine for the Northeast Regional Association of Coastal and Ocean Observing Systems (NERACOOS). Since the beginning of its program in 2005, Bowdoin has operated a two-channel sensor measuring chlorophyll fluorescence and turbidity. Chlorophyll fluorescence, the red light emitted by phytoplankton in response to their absorption of light, is an indicator of their concentration in seawater. Turbidity is a measure of cloudiness due to suspended particles. Observations began on October 22, 2005, and there now are approximately fifteen years of hourly observations. In 2016 Bowdoin began also measuring above-water irradiance and multi-channel chlorophyll fluorescence, beginning with deployment A0136 (deployments are numbered sequentially, A0136, A0137, A0138, etc.).

The focus of this report is the incremental addition of the September 2018 to December 2019 deployments (A0140 and A0141) to the dataset, and some revisions to the irradiance data from deployments A0137-A0139. The quality assurance and analysis methods are described, and bio-optical interpretations of resulting dataset are given.

Sensors

As explained in prior reports (e.g. Roesler 2016) the WETLabs ECO FLNTU two-channel sensor is the standard bio-optical device that researchers have deployed on the mooring since 2005. In order to provide continuous observations with no gaps between deployments, we dedicate two such sensors to the program and swap them on/off the mooring at the start of each

Figure 1. Bowdoin sensors are deployed at a depth of 3 m on Buoy A01 operated by the Northeast Regional Association for Coastal and Ocean Observing Systems (NERACOOS). For reference, Boston, the MWRA outfall tunnel extending offshore from its Deer Island Treatment Plant, the outfall diffuser, Cape Ann, and Cape Cod are also annotated.

deployment, so at all times one is in the field and the other is on shore. The WETLabs factory services and calibrates each of the two FLNTU sensors when it is on shore in between its deployments in the field. On the mooring the FLNTU sensor is integrated into a WETLabs DH4 data handler that provides power to the sensor, controls sampling, archives the raw observations of each hourly burst sampling, and provides hourly mean values to a Campbell data controller (Table 1). The controller incorporates the optical observations, together with those from all other buoy sensors, into a real-time data stream and sends it via cell phone modem or satellite communications to UMaine. There, the data stream is parsed, calibrations are applied to it, and it is made available at the online data portal

Table 1. Components of the optical sensing package on the buoy.

INSTRUMENT	PURPOSE
WETLabs ECO **FLNTU**	Optical sensor, measures chlorophyll fluorescence (at one wavelength) and turbidity, at 3 m depth.
WETLabs ECO **F3WB**	Optical sensor, measures chlorophyll fluorescence at three wavelengths, at 3 m depth.
Satlantic OC507-ICSA	Optical sensor, measures solar irradiance; mounted on the buoy tower.
WETLabs DH4	Data logger, collects and stores data from FLNTU, F3WB, and irradiance sensors; computes mean FLNTU data; transmits means to Campbell Data Logger, which transmits it in real time to the University of Maine where it is relayed to NERACOOS and posted online.

http://gyre.umeoce.maine.edu/data/gomoos/buoy/html/A01.html and sent to NERACOOS, who also presents it online in real time at their website www.neracoos.org.

Additional bio-optical sensors are deployed, in a stand-alone configuration integrated into the same DH4, but their data are not transmitted in real time due to limitations of the Campbell software. There is a significant time lag for processing of these additional data, as instruments must be recovered from the mooring, transported to Bowdoin, cleaned, downloaded and post-processed. However, it is then possible to recover the full data set from the FLNTU, comprised of a one-minute sample burst each hour, with each burst consisting of approximately 60 readings. These values are analyzed to ensure the mean value reported in real time is a robust estimate of the sample burst observations, by comparison to their median and standard deviation.

In addition to the FLNTU, optical sensors include, first, a multi-channel fluorometer which is a custom made WETLabs ECO Triplet sensor FL3-WB that consists of 3 excitation channels (435nm, 470nm, 532nm) and one emission channel (695nm) to detect chlorophyll fluorescence stimulated by different accessory pigments in phytoplankton that absorb in the three wavelength bands. This sensor has been used to detect changes in phytoplankton community composition in Maine Lakes (Proctor and Roesler 2010), the Arabian Sea (Thibodeau et al. 2014), the western Mediterranean Sea (Roesler et al. 2017) and in eastern Casco Bay (http://bowdoin.loboviz.com). Phytoplankton community composition is the relative abundance of different types of phytoplankton present together in seawater, which varies from location to location and temporally, and is an important aspect of water quality and ecological conditions. Chlorophyll concentration is a useful measure of phytoplankton concentration but does not capture phytoplankton community composition.

Second, a Satlantic OC507-ICSA seven-channel irradiance sensor is deployed on top of the mooring and connected to the subsurface DH4 via a long cable through the well of the float.

This sensor is factory calibrated and provides hourly estimates of incident downwelling irradiance E_D ($\mu W\ cm^{-2}$). Third, a Satlantic OC507-ICSW-R10 seven-channel in-water radiance sensor with 10^o solid angle detection was deployed in a downward viewing configuration to measure nadir upwelling radiance ($\mu W\ cm^{-2}\ sr^{-1}$; sr is steradian) at the depth of the bio-optical frame (3m). This sensor was also factory calibrated. There are no anti-biofouling capabilities for this sensor and there was a significant loss of data due to fouling. It is no longer deployed.

Instrument Calibration. Recent work has concluded that the factory calibrations of the WETLabs ECO model chlorophyll fluorometers are biased by a factor of 2 (Roesler et al. 2017). For this reason, the laboratory calibration for the chlorophyll fluorometer has always been implemented for sensors on Buoy A01, instead of factory calibrations. All fluorometers are calibrated in the lab prior to deployment using ten dilutions of a monospecific culture of the diatom *Thalassiosira pseudonana* (Proctor and Roesler 2010). The culture is grown in nutrient replete L1 media at an irradiance that maximizes growth rates (i.e. ~300 $\mu Ein\ m^{-2}\ s^{-1}$) and minimizes pigment packaging due to low light acclimation. The culture is harvested during exponential growth with maximal extracted chlorophyll concentrations between 20 mg m^{-3} and 50 mg m^{-3}. This approach to calibration provides a transfer function between sensors and between a single sensor over time, accounting for variations in sensor gain, and also provides conversion of the signal from digital counts (millivolts) to biogeochemical units (mg m^{-3}). Because the excitation wavelength (470 nm) does not directly stimulate chlorophyll fluorescence, it is not possible to calibrate with a standard dilution of purified pigment. In vivo fluorometers take advantage of the energy transference between accessory pigments in the light harvesting complexes to chlorophyll *a* by stimulating accessory pigment absorption at 470 nm. While the fluorescence yield (fluorescence per extracted chlorophyll) varies between species, as a function of environmental acclimation, growth phase, and non-photochemical quenching, each of these sources of variability can be assessed on long-term time scales of observations and thus the impacts can be minimized or exploited for further information (Roesler and Barnard 2013).

Detailed explanation of the 6-step post-processing of the real-time data for quality control

The following steps are necessary to maintain the high quality of the dataset.

Step 1. Quality assurance on times recorded by the irradiance sensor. While the fluorometer/turbidity and the 3-channel fluorometer sensors record timestamps aligned with those of the buoy real time data stream, the irradiance sensor does not. It was discovered that there are some variations in the timing of the irradiance sensor samples, as well as some jumbled transmitted data packets. As a first-cut solution, the raw archived data stream was binned (ignoring its timestamps) into hourly means, medians and standard deviations (120-burst samples within the 2-minute sampling window, Figure 2A) and assigned timestamps uniformly distributed across the entire deployment. Low irradiance values, between zero and the method detection limit (MDL), indicate darkness and were used to identify nighttime hours

(Figure 2B). This enabled identification of erroneous times, such as the nighttime values observed during daylight hours in February. Correct timestamps were then assigned using each interval of more than 4 sequential dark readings as one night-time interval. The midpoint of each dark interval was assigned the hour of midnight. Values between midnights were then assigned to 24 uniformly distributed hourly timestamps. In this way, the irradiance measurements were given correct timestamps consistent with those of the other sensors (Figure 2C).

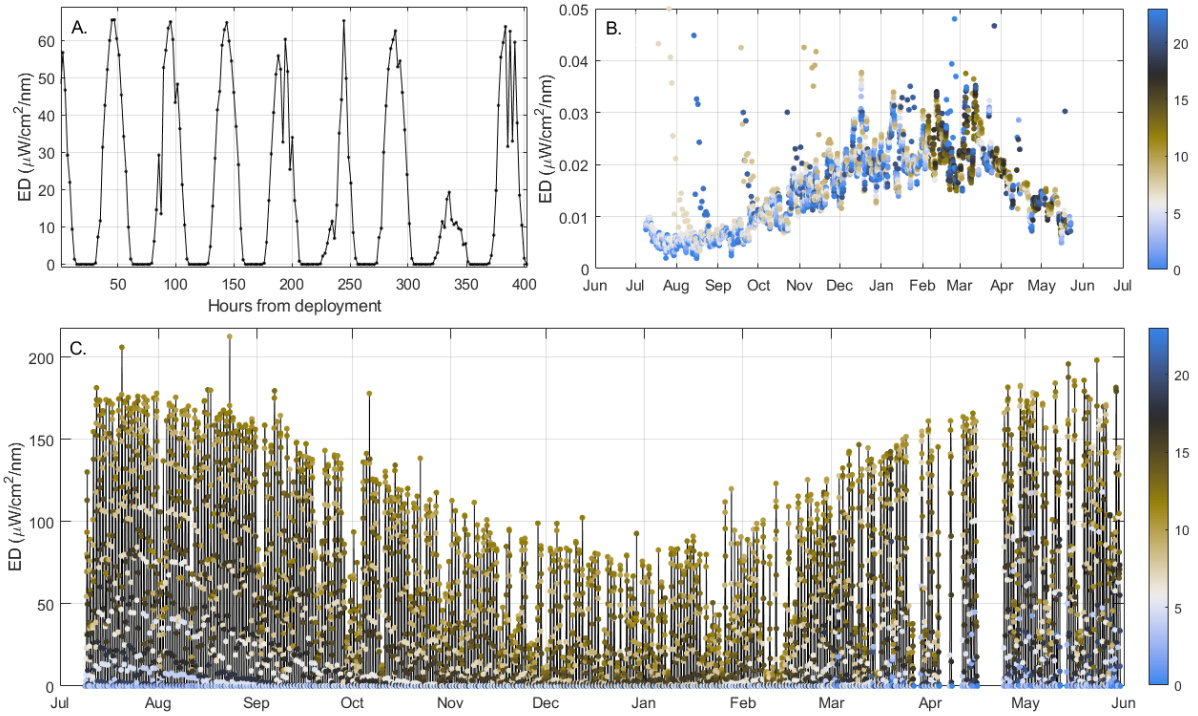

Figure 2. A. Observed median-binned burst samples of solar irradiance (440 nm) from short initial portion of deployment. B. Time series hourly observations interpolated to buoy real time data stream timestamps and color-coded by local hour; vertical axis the same as in A, but only the range from zero to +MDL to restrict to nighttime observations. C. Final results with correct timestamps, color-coded by local hour, deployment A0140, vertical axis same as in A.

Step 2. Correction for sensor drift. Offsets can occur between recovery/deployment of sensors. Bowdoin evaluates these offsets by post recovery calibration or by identification of offset relative to prior and subsequent deployments (Figure 3). It is challenging to identify offsets in the FLNTU sensor signals due to the intense biofouling that occurred at the end of A0140 in both chlorophyll fluorescence and turbidity (Figure 3A, C and E). The shuttered F3WB sensors are much less vulnerable to biofouling and exhibited no offset between deployments for all three fluorescence channels (Figure 3 B, D, and F).

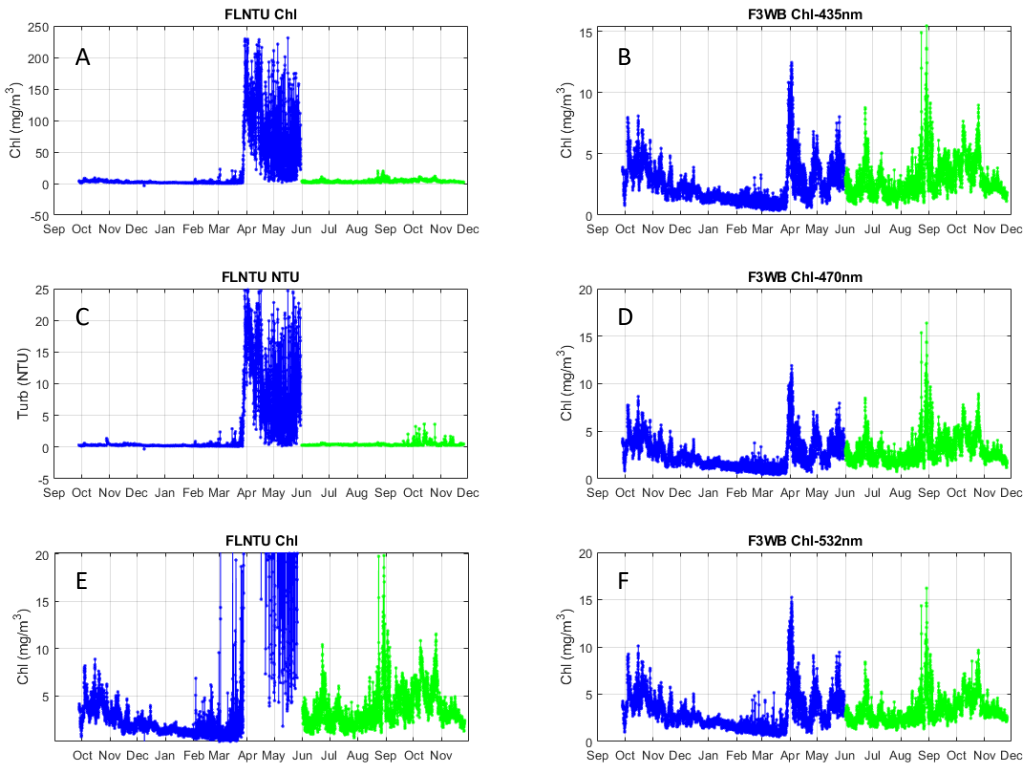

Figure 3. Time series of the A0140 (blue) and A0141 (green) deployments of hourly observations of chlorophyll fluorescence and turbidity from the FLNTU sensor (A and C, respectively) and chlorophyll fluorescence from the three channels of the F3WB (B, D, and F, respectively). The FLNTU chlorophyll fluorescence time series on an expanded scale is in E.

Comparison between the chlorophyll fluorometers (using comparable channels with excitation at 470 nm and 695 nm emission) on the two sensors are performed to quantify inter-calibration differences. For the non-biofouled observations during A0140, the two sensors yielded comparable estimates of chlorophyll concentration (Figure 4A). However, during A0141 the FLNTU chlorophyll sensor underestimated the F3WB chlorophyll estimate by approximately 25% (green symbols in Figure 4B). The FLNTU results were flagged and the FLNTU values corrected using a type II regression that incorporates the variance in each hour mean to estimate the slope and intercept (cyan symbols in Figure 4B).

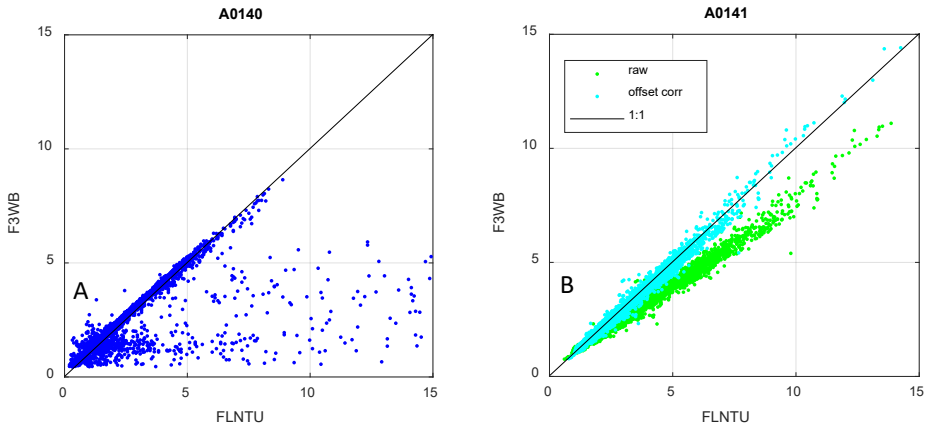

Figure 4. Relationship between simultaneous chlorophyll concentration estimates measured with the F3WB channel 2 fluorometer and the FLNTU fluorometer for A. A0140 (blue symbols) and B. A0141 (green symbols). The black line is one-to-one line. The best fit type II regression was computed for the A0141 observations and applied to the FLNTU observations to yield the corrected chlorophyll concentration estimates (cyan symbols).

The noontime irradiance spectra (Figure 5A) reveal evidence of inter-calibration errors in that the spectral shape of the curves are not consistent with what is measured with a calibrated hyperspectral radiometer deployed routinely from shipboard in eastern Casco Bay. The 555 nm channel is typically the most robust in terms of signal to noise and thus this channel was used to compute the spectral corrections for each deployment (Figure 5B).

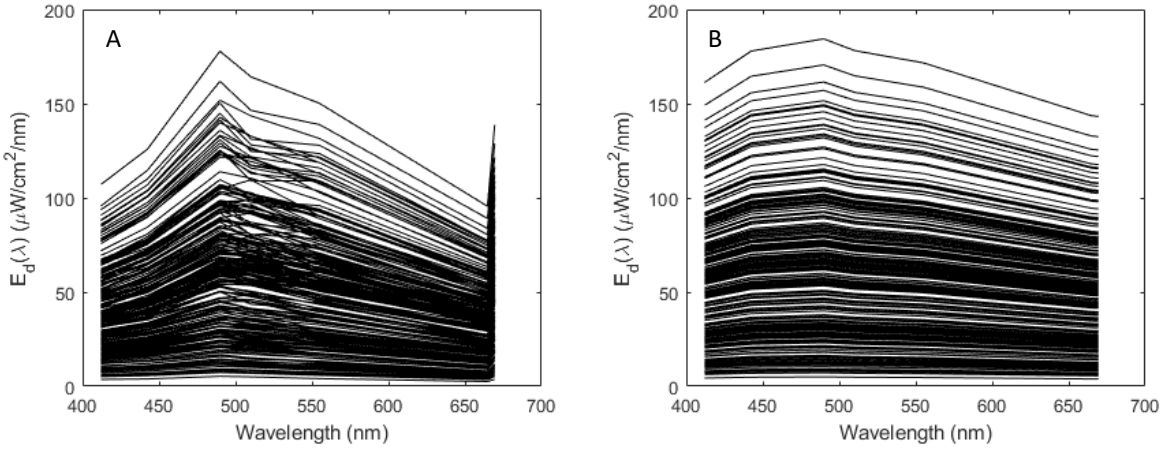

Figure 5. Noontime downwelling spectral irradiance scans, one line per day, A. measured at the top of the mooring spar and B. corrected for spectral offsets.

Downwelling irradiance observations also varied between deployments (calibration offsets, Figure 6A). The time series of monthly maximal values represent clear sky observations. This

time series was compared to that obtained from a moored hyperspectral radiometer in eastern Casco Bay which is intercalibrated with the ship-deployed sensor described above. The offsets between deployments were computed based upon the time series of clear-sky maximal observations and the offsets between deployments were corrected and flagged (Figure 6B).

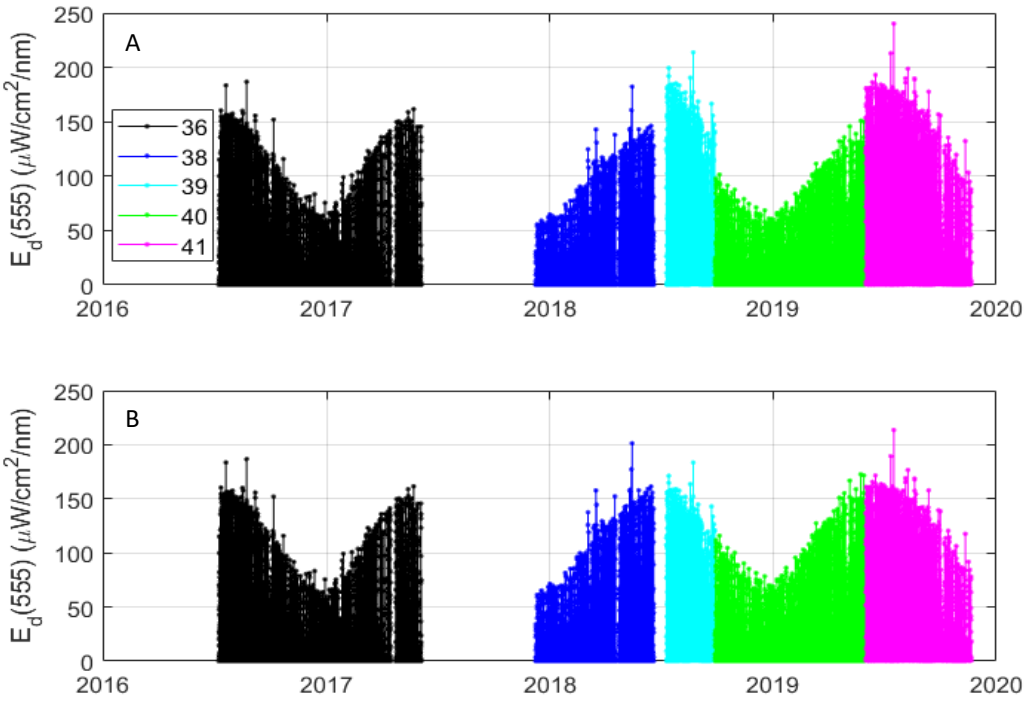

Figure 6. Time series of downwelling irradiance at 555 nm for deployments A0136 (black), A0138 (blue), A0139 (cyan), A0140 (green) and A0141 (magenta) for A. raw hourly observations and B. hourly observations post offset correction. Gaps are due to bio-fouling.

Step 3. Removal of biofouled data. Biofouling manifests as a logarithmic signal increase leading to out-of-standard range or to saturating values. Biofouling takes two forms (Figure 7): a smooth signal increase associated with biofilm growth or an extreme hour-to-hour variability due to structural growth on the sensor such as seaweeds that contaminate both the fluorescence and turbidity signals as they waft into the optical sensing volume ("frondular biofouling"). Bowdoin flags biofouled observations as either biofilm or structural based upon the pattern of anomalous observations and removes them from the data stream.

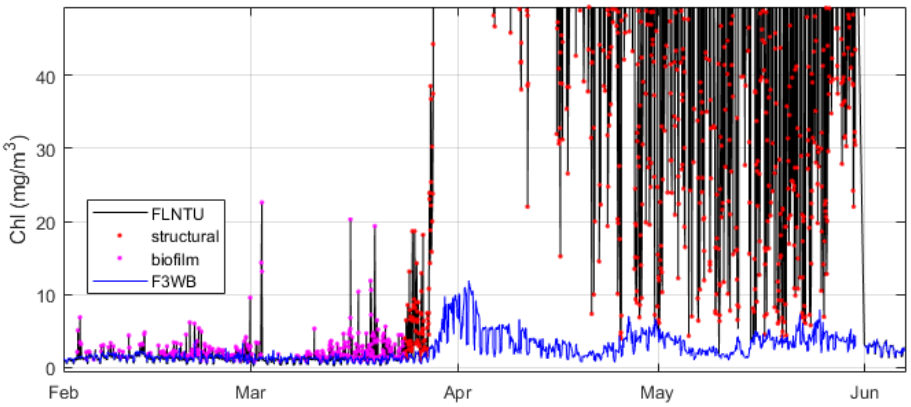

Figure 7. Time series of 2019 hourly observations of chlorophyll fluorescence from the unshuttered FLNTU sensor (black) and the shuttered F3WB sensor (blue) for A0140 and the beginning of A0141). For the FLNTU the onset of biofilm biofouling (magenta symbols) was observed in February and the onset of structural (red symbols) was observed late March.

Step 4. Identification, flagging, and correction of chlorophyll fluorescence observations impacted by non-photochemical quenching (NPQ). High levels of incident irradiance induced non-photochemical quenching (NPQ) in the chlorophyll fluorescence observations within the near-surface waters of the euphotic zone. The effect decreases exponentially with depth as the in-water irradiance also decreases exponentially. The onset of NPQ at the surface occurs as early as dawn and recovery from NPQ is just prior to sundown, on average within 7 hours of midnight (Figure 8A). These hours of NPQ are flagged and the data removed from the data stream.

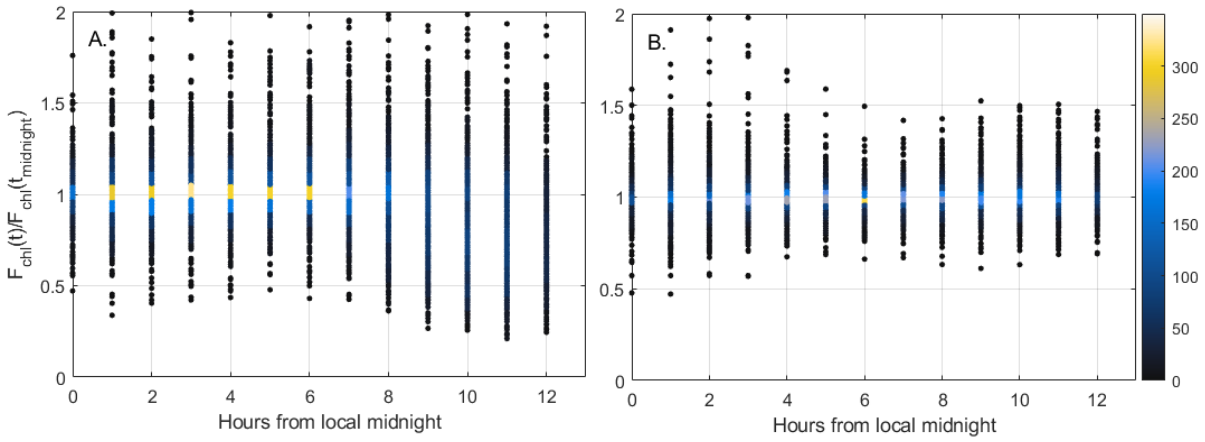

Figure 8. Heatmap (number of observations color-coded) of ratio of hourly (A) raw and (B) NPQ-corrected chlorophyll fluorescence to adjacent midnight fluorescence as a function of hours from local midnight. A ratio of one indicates no NPQ. Scatter indicates sub-diel patchiness in phytoplankton populations.

In order to recover what is nearly 50% of the hourly observations, the published method of Carberry et al. (2019), is used to estimate the chlorophyll fluorescence during the hours of observed NPQ. The process is briefly described below. The raw hourly chlorophyll fluorescence and solar irradiance timeseries are used to identify daytime (quenched) and nighttime (unquenched) chlorophyll fluorescence observations (Figure 9A). Tidal currents measured at the surface near the fluorometer with the Aanderaa current meter are rotated from north-south and east-west components into alongshore and cross-shore components. The alongshore component is then used to identify slack current and specifically the hours of high and low tide conditions (Figure 9B). The time series of high and low tide conditions that occur during nighttime hours are used to identify the unquenched chlorophyll concentrations associated with the high and low tide endmembers (presumed different populations of phytoplankton). Because the solar cycle is 24 hours and the tidal day is approximately 24 hours and 48 minutes, there are days for which there is no high or low tide during the hours of unquenched fluorescence. These values are interpolated (Figure 9C). Once the entire cycle of nighttime high and low tide unquenched fluorescence is obtained, the cycle of the tide between high and low is treated as a cosine function to retrieve the estimate of chlorophyll fluorescence for each hour during the daytime (Figure 9D). This estimate assumes that the variations in chlorophyll fluorescence will be primarily determined by conservative mixing between the high and low tide populations. Differences between observed and modeled estimates will be due to NPQ (during the day) and non-conservative processes or variations in populations that are small compared to the scale of tidal advection.

Although the Cape Ann mooring does not undergo the same tidal dynamics as the coastal embayment for which the method was developed, there is a clear semidiurnal tidal signal in the surface currents and the fit to nighttime fluorescence indicates that much of the observed fluorescence variability is due to tidal advection. Where the fit is not robust it is an indication that the conservative mixing assumption is weak and/or that there is sub-diel patchiness in the phytoplankton populations that flow past the mooring. As a check on the removal of NPQ, the ratio of hourly corrected chlorophyll fluorescence to adjacent midnight observations does not exhibit a dependence on daylight hours (Figure 8B).

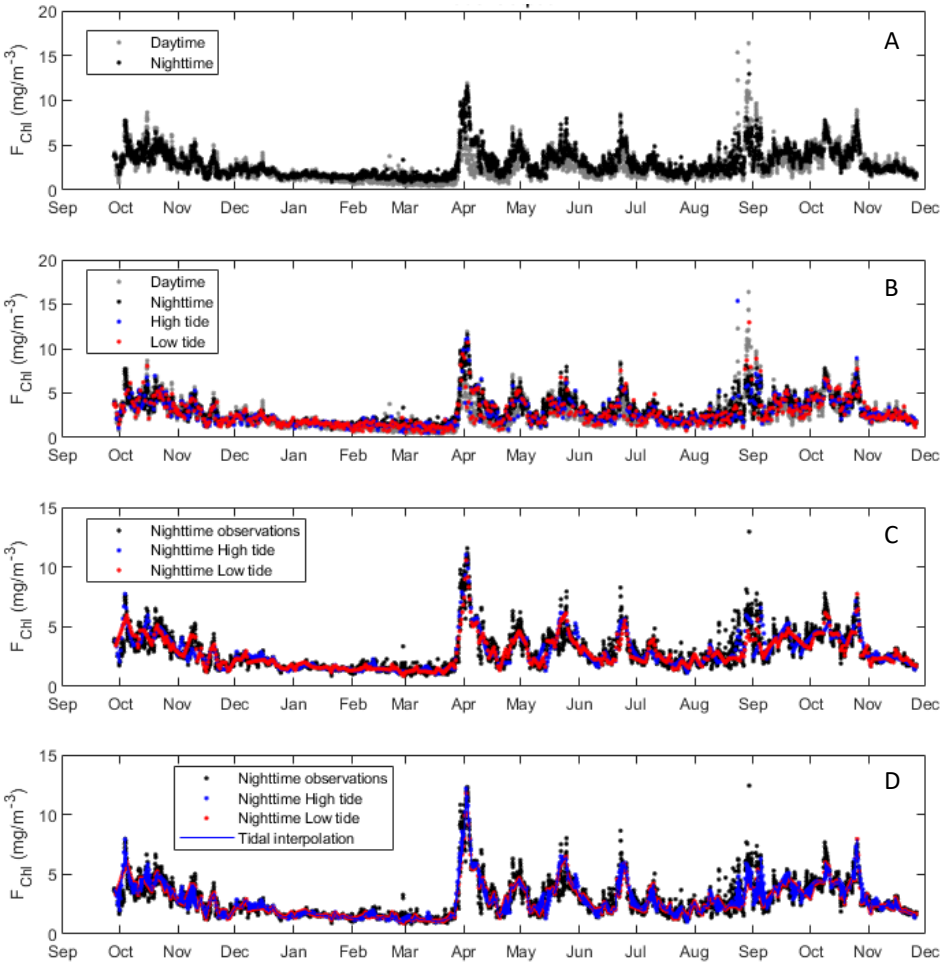

Figure 9. Timeseries of 2018-2019 hourly observations of chlorophyll fluorescence during deployments A0140-A0141 by the shuttered F3WB sensor, distinguished by A. daytime and nighttime, B. high and low tide, C. nighttime high and low tide, D. tidal interpolation between unquenched high and low tide endmembers.

Step 5. Removal of single value outliers (SVOs). SVOs are identified differences between successive consecutive measurements that exceed the coefficient of variation and are in excess of 15 mg/m^3 (chlorophyll) or 3 NTU (turbidity). Single Value Outliers are flagged and removed from the data streams (Figures 10 and 11).

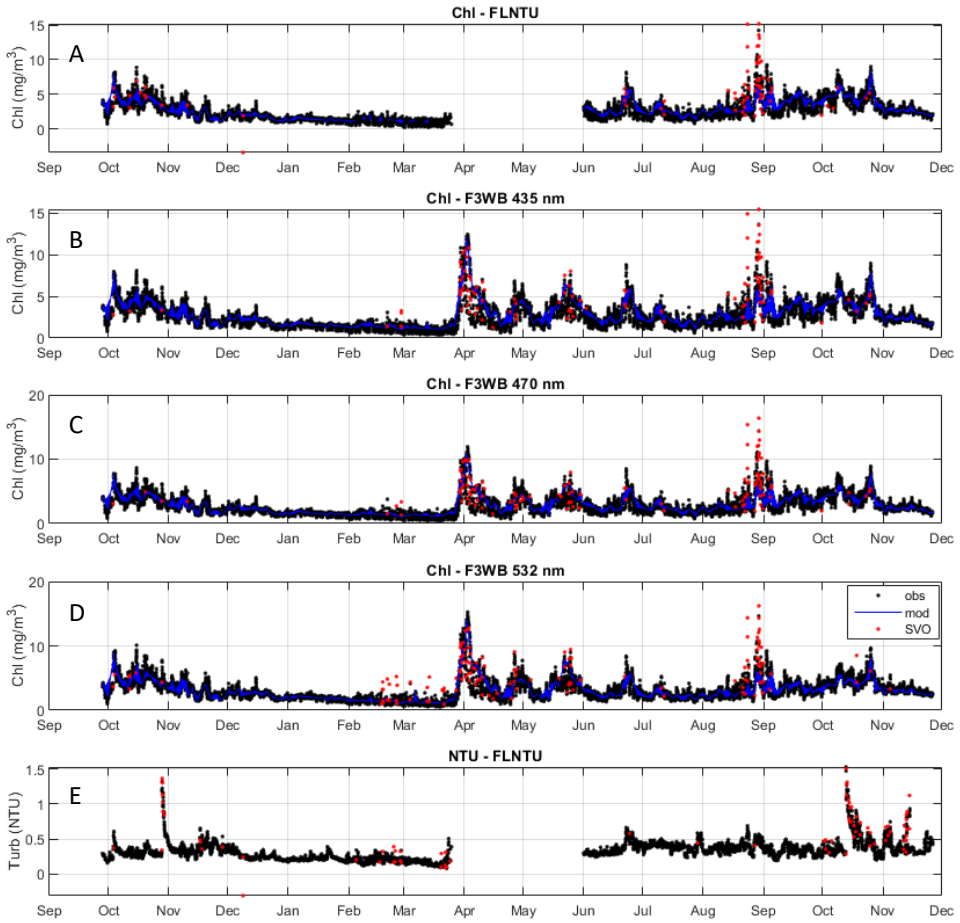

Figure 10. Time series observations of 2018-2019 hourly (A-D) chlorophyll fluorescence (with NPQ-corrected results, "mod" in legend) and (E) turbidity from the F3WB and FLNTU sensors during A0140 and A0141 with data points for SVO identified. Gaps in FLNTU due to biofouling.

Step 6. Identify values below minimum detection levels. The minimum detection levels (MDLs) of the chlorophyll, turbidity, irradiance and radiance sensors are 0.05 mg/m^3, 0.05 NTU, 0.06 μW m^{-2} and 0.0003 μW m^{-2} sr^{-1}, respectively. Observations below -1*MDL are flagged and removed. Values between -1*MDL and 0, and those between 0 and +1*MDL are independently flagged, for convenience of entering the data in the MWRA database where different value qualifiers are applied to the two ranges (Figures 10 and 11). The negative values are not removed because removing negative values within an MDL of zero leads to positive biasing of the observed data (Thompson 1998).

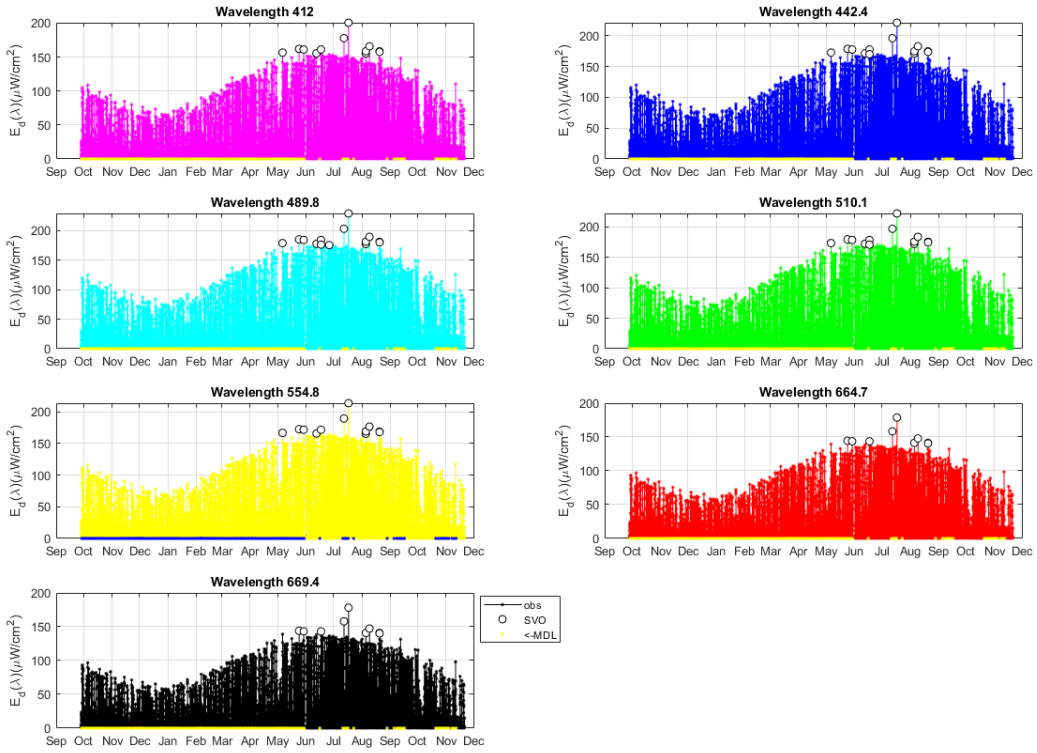

Figure 11. Time series observations of 2018-2019 hourly downwelling irradiance at 7 wavelengths during A0140 and A0141 with data points for Single Value Outliers (SVOs; circles) and values below the Method Detection Limit (MDL; blue for wavelength 554.8 nm; yellow for other wavelengths) identified.

Data products provided

In order to give a clear sequence of observations, flagging and correction steps, we provide hourly data arrays including each stage of the post-processing. These are also helpful for optimization of correction schemes for biofouling and NPQ.

Separate data files are submitted for:

- the chlorophyll (Chl) and turbidity (NTU) sensors of the FLNTU,
- each channel of the calibrated ECO F3WB chlorophyll fluorometer (F1 through F3),
- the 7-channel irradiance (ED7).

The Appendix provides data string formats:

Table A1 provides the data string for hourly chlorophyll fluorescence data obtained from the ECO FLNTU and FL3-WB sensors.

Table A2 provides the data string format for the hourly turbidity.

Table A3 provides the data string format for the hourly downwelling irradiance and upwelling radiance data files.

Table A4 provides a list of the data file names, descriptions, units and array sizes.

The data arrays provided have the Matlab binary storage “mat” file format.

Results and Discussion

Time series bio-optical observations

The time series bio-optical observations from the FLTNTU span 2005 through November 2019 while the observations from the F3WB and irradiance sensors (deployments A0137-A0141) span from June 2017 to November 2019 (Figure 12). **The most recent deployments exhibit lower variability in both chlorophyll and turbidity compared to most previous years.**

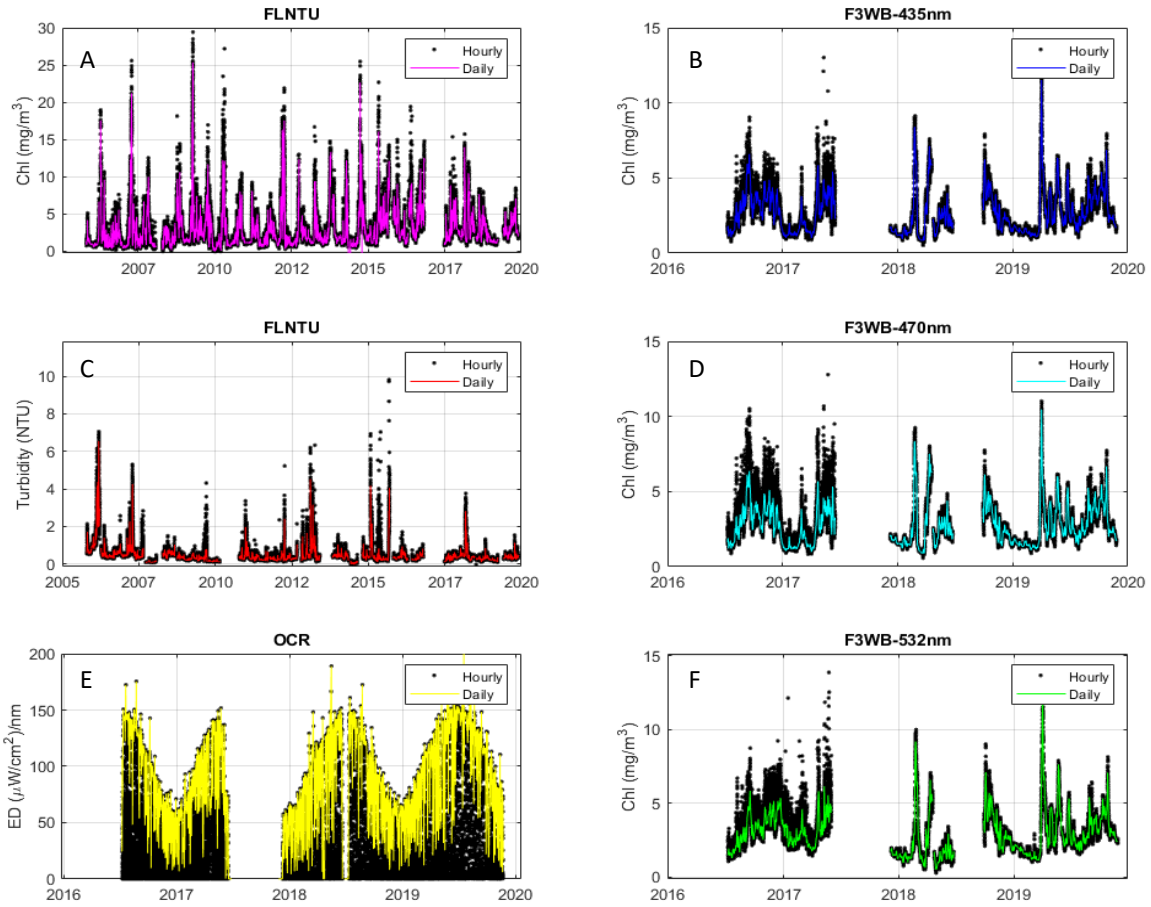

Figure 12. Time series hourly (black symbols) and daily (colored lines) observations of chlorophyll fluorescence (A, B, D, F), turbidity (C), and solar irradiance (E). Daily values represent medians for all but irradiance which is daily maximal value. Gaps due to biofouling.

The daily climatological values for the bio-optical time series (Figure 13) clearly show that there is a distinct and narrow spring bloom that peaks in early April and a broad fall bloom of slightly lower magnitude that spans September through November. Minimal chlorophyll concentrations are observed during the winter (late December through March) and summer (July). The pattern

over the last 4 years of F3WB observations indicates that a spring bloom can occur as early as February and that up to four separate spring blooms can be observed. The fall bloom pattern is much less variable, with a longer duration and a similar magnitude in peak concentration.

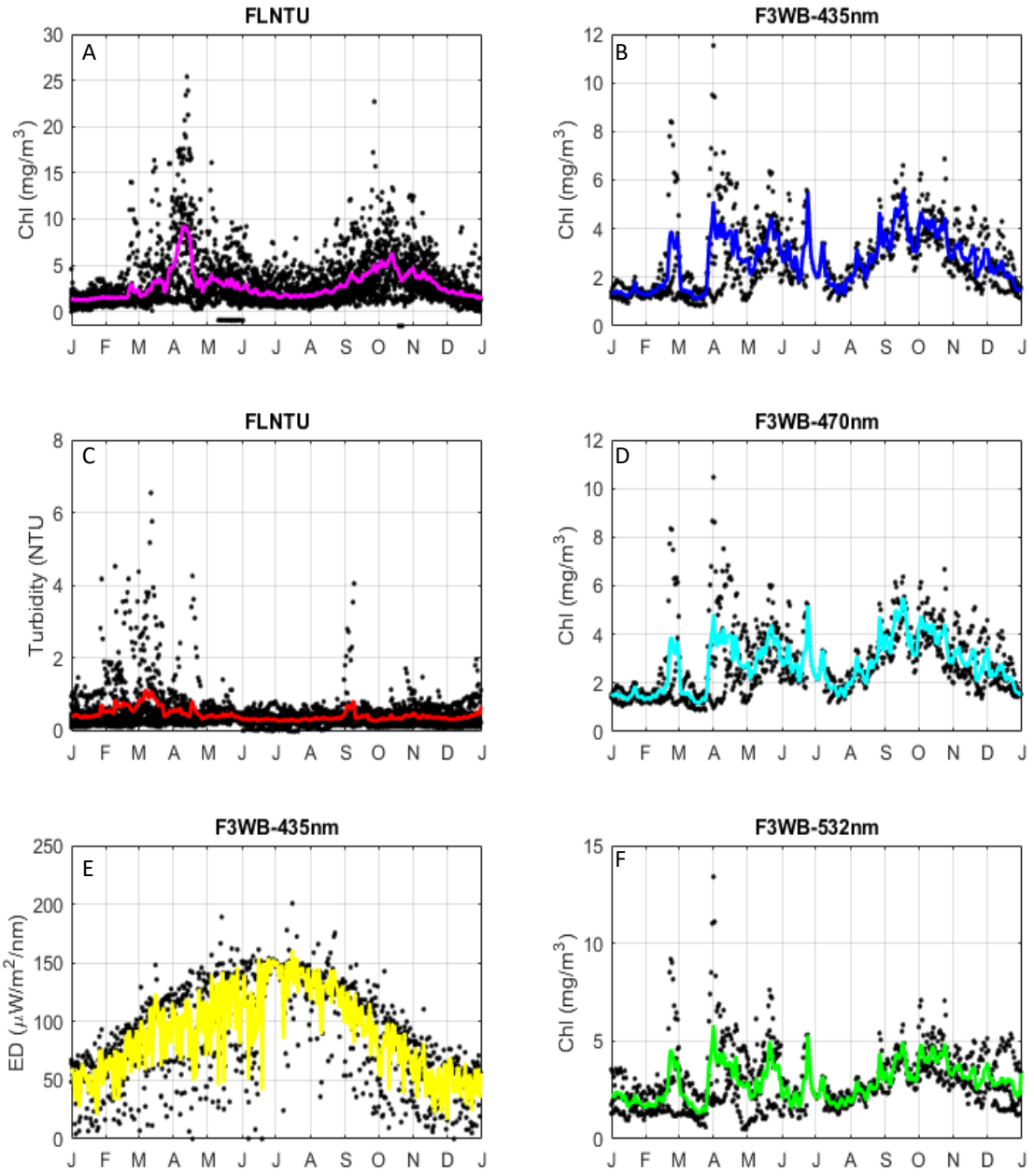

Figure 13. Daily observations (black symbols) and climatological means (colored lines) for the bio-optical time series (Figure 12).

Monthly climatological means for the bio-optical time series are shown in Figure 14. For the 15-year data sets, the spring bloom occurs in April and the fall bloom peaks in October. The magnitude of the spring bloom is much more variable than that of the fall bloom and slightly smaller (Figure 14A). The summer minimum is more variable in magnitude than the winter minimum. The monthly means for the past four years are slightly different from the longer term monthly patterns (Figure 14 B, D, F) with the peak of the spring bloom occurring in May and both blooms having more extended durations. The seasonal pattern in turbidity is essentially flat through the year (Figure 14C), however, there is substantial variability January through April when winter storms drive events in increased turbidity. September also appears to be a month of higher variability. The monthly pattern in solar irradiance (Figure 14E) reveals peak irradiance in July, minimal in December, with June exhibiting the most variability. The hourly patterns in irradiance indicate this is consistent with increased cloudiness late spring to early summer compared to the summer and fall months.

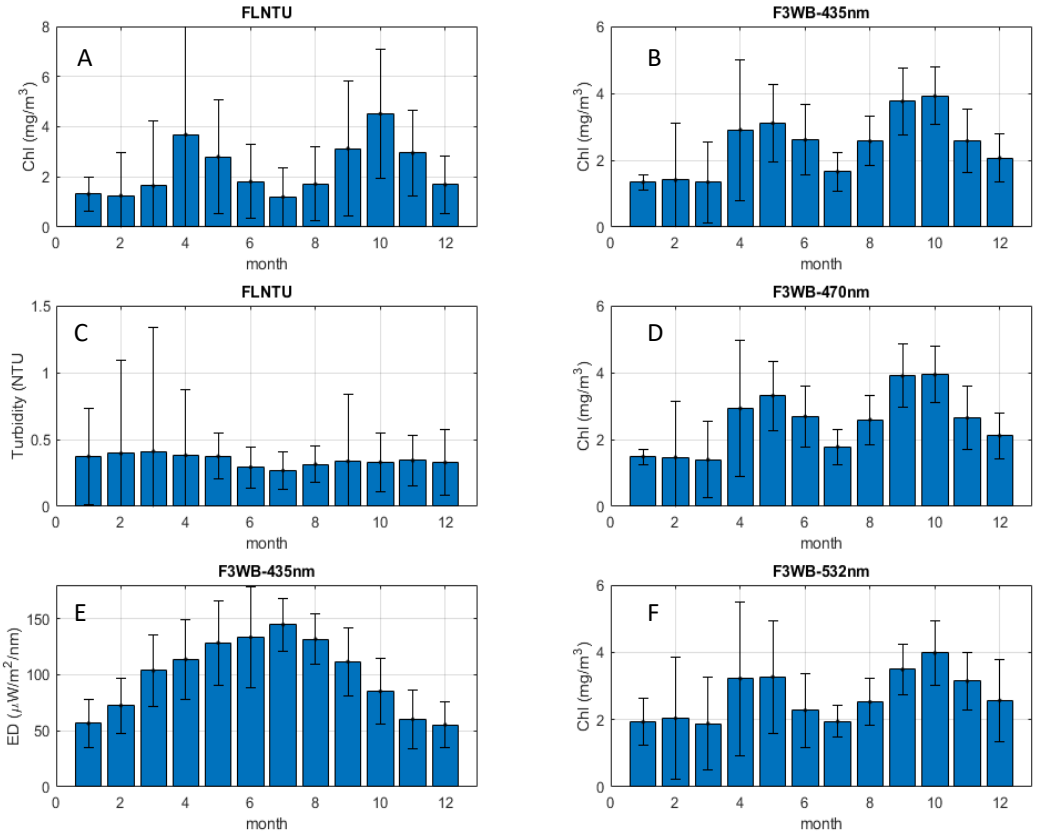

Figure 14. Monthly median values of chlorophyll fluorescence (A, B, D, F), turbidity (C), and solar irradiance (E). Error bars indicate standard deviation.

Annual median values of the bio-optical observations reveal a trend of increasing chlorophyll from 2006-2009, an interval of relatively constant annual chlorophyll from 2010-2014, and a higher chlorophyll concentration from 2015-2019 (Figure 15A). The annual mean pattern in turbidity exhibits a decrease from 2005-2009 followed by more uniform mean values over the past decade (Figure 15B). Three years (2006, 2013 and 2015) have exhibited the strongest variability. There is not sufficient length of observations to interpret the irradiance or F3WB observations.

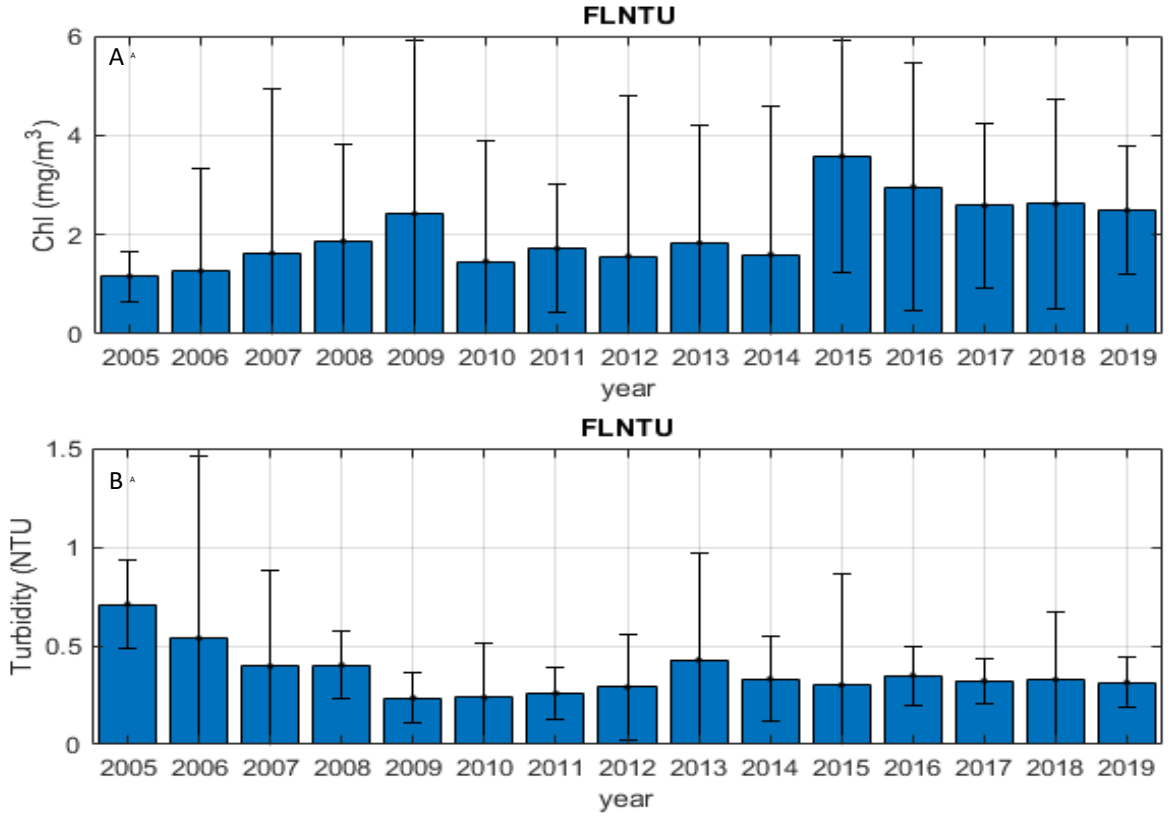

Figure 15. Annual medians of daily values in Figure 11 of A. chlorophyll concentration and B. turbidity, error bars represent standard deviations.

The pattern in annual median chlorophyll concentrations can be driven by high peak concentrations during blooms, longer blooms or overall higher sustained concentrations. A Hovmöller diagram (Figure 16) is used to identify which factor may be at play. The dotted lines are used to identify the timing of the onset and decline of the spring and fall blooms. Results suggest that the spring bloom is occurring earlier, and its duration is increasing. It also appears that the fall bloom duration is weakly increasing and becoming less peaked. 2015 was the year of maximal median chlorophyll concentration; it appears that the chlorophyll concentration remained high throughout the summer and since that time the duration of the summer minimum has decreased. These long-term variations and trends are most likely due to regional changes in temperature and salinity stratification (Thomas et al. 2017).

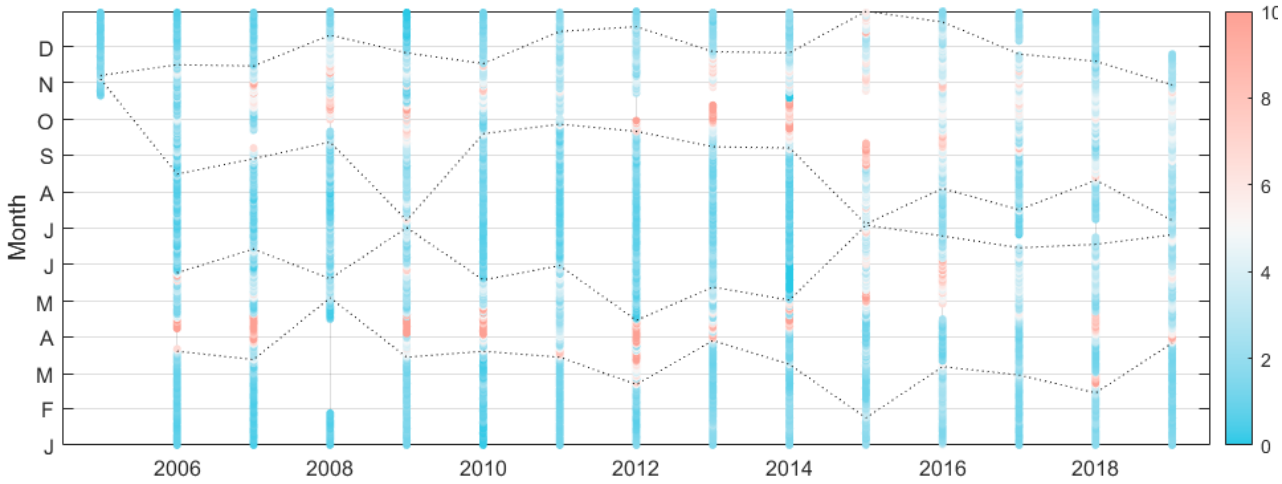

Figure 16. Hovmöller diagram of chlorophyll concentration over the entire bio-optical times series at Buoy A01. Units of colorbar are mg chl/m^3. Dotted lines represent the extent of spring and fall blooms where chlorophyll exceeds 3 mg/m^3.

Multi-channel fluorescence as indicator of evolving phytoplankton community composition

The WETLabs FL3-WB, three-excitation single emission chlorophyll fluorometer, yields time series of the intensity of the chlorophyll fluorescence in response to each excitation wavelength that varies as the absorption coefficient at that wavelength varies, and thus as the pigment composition varies. Thus, fluorescence ratios are comparable to pigment absorption ratios. Raw fluorescence for each channel is calibrated to the diatom *Thalassiosira pseudonana*, thus ratio values of 1.0 indicate diatom domination. Variations from 1.0 indicate variations in pigment composition relative to the diatom signal (Proctor and Roesler, 2010; Thibodeau et al. 2014).

The A0140-A0141 F3WB time series are bracketed by two fall blooms and include a winter minimum and 4 distinct spring blooms from April through June (Figure 17A). The associated fluorescence ratios (Figure 17B) identify a single phytoplankton community from October 2018 through January 2019. The winter minimum from January through March is a second community. Each of the four blooms appears to vary compositionally and the onset of the fall bloom 2019 is compositionally different from the decline of the 2018 and 2019 fall blooms.

The ratio-ratio comparison (Figure 17 C and D) clarifies that the October communities are dominated by diatoms, the winter community has a fluorescence fingerprint that has been associated with haptophytes and cyanobacteria, while the April bloom is likely dominated by dinoflagellates. The onset of the fall bloom in early September is consistent with diatoms, followed by cryptophytes in late September to early October, evolving back to the winter population associated with haptophytes and cyanobacteria. If the opportunity becomes available to collect water samples for HPLC pigment analyses by Bowdoin, it would be possible to validate the fluorescence fingerprint time series.

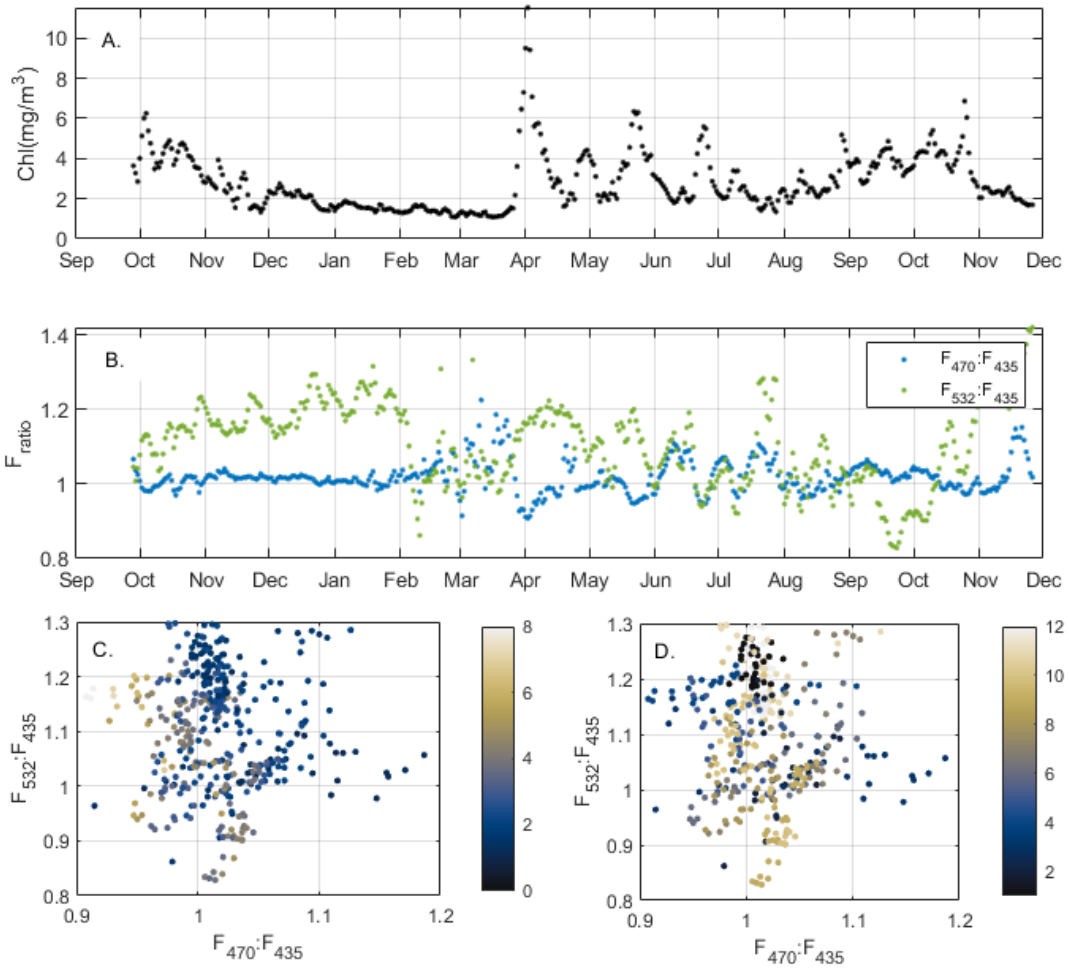

Figure 17. Time series (September 2018 to December 2019) of daily median values of A. chlorophyll concentration and B. fluorescence ratios. Corresponding daily-median fluorescence ratio-ratio values color coded by C. chlorophyll concentration and D. month.

References

Carberry, L., C. S. Roesler, and S. L. Drapeau. 2019. Correcting in situ chlorophyll fluorescence time series observations for non-photochemical quenching and tidal variability reveals non-conservative phytoplankton variability in coastal waters. Limnol. Oceanogr. Methods. DOI: 10.1002/lom3.10325

Proctor, C. W., and C. S. Roesler. 2010. New insights on obtaining phytoplankton concentration and composition from in situ multispectral Chlorophyll fluorescence. Limnology and Oceanography: Methods **8:** 695-708.

Roesler, C. S. 2016. In Situ Chlorophyll Fluorescence Observations on NERACOOS Mooring A01: Revised Data Flagging and Changing Phenology. Boston: Massachusetts Water Resources Authority. Report 2016-15. 11 p. http://www.mwra.state.ma.us/harbor/enquad/pdf/2016-15.pdf

Roesler, C. S. and A. H. Barnard, 2013. Optical proxy for phytoplankton biomass in the absence of photophysiology: Rethinking the absorption line height. Methods Oceanogr. 7: 79-94. Doi:10.1016/j.mio.2013.12.003 .

Roesler, C. S., J. Uitz, H. Claustre, E. Boss, X. Xing, E. Organelli, N. Briggs, A. Bricaud, C. Schmechtig, A. Poteau, F. D'Ortenzio, J. Ras, S. Drapeau, N. Haëntjens, and M. Barbieux, 2017. Recommendations for obtaining unbiased chlorophyll estimates from in situ chlorophyll fluorometers: A global analysis of WET Labs ECO sensors. Limnol. Oceanogr. Methods, 15: 572–585. doi:10.1002/lom3.10185.

Thibodeau, P. S., C. S. Roesler, S. L. Drapeau, S. Prabhu Matondkar, J. I. Goes, and P. J. Werdell. 2014. Locating Noctiluca miliaris in the Arabian Sea: An optical proxy approach. Limnology and Oceanography **59:** 2042-2056.

Thomas, A.C., Pershing, A.J., Friedland, K.D., Nye, J.A., Mills, K.E., Alexander, M.A., Record, N.R., Weatherbee, R. and Henderson, M.E., 2017. Seasonal trends and phenology shifts in sea surface temperature on the North American northeastern continental shelf. *Elem Sci Anth*, 5, p.48. DOI: http://doi.org/10.1525/elementa.240

Thompson, M. (1998). Perspective: Do we really need detection limits? Analyst 123(2): 405-407.

Acknowledgements

The work in this report represents significant contributions by many people, often behind the scenes. Collaboration with Neal Pettigrew on the design and implementation of the observing system has persevered for over two decades. The Physical Oceanography Group at University of Maine has worked tirelessly to integrate the optical observing system into their mooring infrastructure, and to deploy and recover on a timescale that supports a successful bio-optical program. Susan Drapeau at Bowdoin College is responsible for the day-to-day work required for obtaining high quality bio-optical data including sensor calibration, maintenance, and integration, and maintaining the data archive. Finally, Sally Carroll and Dan Codiga at MWRA provided insightful reviews and contributed important suggestions to improve this report and make it accessible to a broad audience. All the work presented is a result of support from MWRA.

Appendix. Data file formats.

Table A1. Format of the hourly observational data file for chlorophyll fluorescence data arrays, including those derived from FLNTU and FL3-WB sensors.

Column	ID	Value/Range	Comment
1	Year	2005-2019	
2	Month	1-12	
3	Day	0-31	
4	Hour	0-25	
5	Minute	0-60	
6	Second	0-60	
7	Date.Time	732607 - 737335	Matlab format
8	Raw Fchl	-1.63 – 162.56	Raw hourly mean
9	Flag_Offset	0, 1	Between deployments
10	Fchl_corr_offset		Corrected for offsets
11	Flag_Biofouling1	0, 1	Biofilm
12	Flag_Biofouling2	0, 1	Structural
13	Fchl_corr_biofouling	NaN	Values removed
14	Flag_NPQ	0, 1	NPQ
15	Fchl_corr_NPQ	-0.04 28.6	Values corrected (Carberry et al. 2019)
16	Flag_SVO	0, 1	Single value outlier
17	Fchl_corr_SVO	NaN	Values removed
18	Flag_MDL1	0, 1	< - Method detection level (MDL)
19	Flag_MDL2	0, 1	-MDL to 0
20	Flag_MDL3	0, 1	0 to +MDL
21	Fchl_corr	-0.04 to 29.47 /NaN	Cumulative removal/correction
22	Deployment	15 – 39	Deployment number
23	ECO-FLNTU S/N	001-9999	Sensor serial number, FLNTU

Table A2. Format of the hourly observational data file for Turbidity.

Column	ID	Value/Range	Comment
1	Year	2005-2019	
2	Month	1-12	
3	Day	0-31	
4	Hour	0-25	
5	Minute	0-60	
6	Second	0-60	
7	Date.Time	732607 - 737335	Matlab format
8	Raw Turbidity	-0.59 to 25.95	
9	Flag_Offset	0, 1	
10	Turb_corr_offset		Corrected for offsets
11	Flag_Biofouling1	0, 1	Biofilm
12	Flag_Biofouling2	0, 1	Structural
13	Turb_corr_biofouling	NaN	Values removed
14	Flag_SVO	0, 1	Single value outlier
15	Turb_corr_SVO	NaN	Values removed
16	Flag_MDL1	0, 1	< - Method detection level (MDL)
17	Flag_MDL2	0, 1	-MDL to 0
18	Flag_MDL3	0, 1	0 to +MDL
19	Turb_corr	-0.05 to 9.81 /NaN	Cumulative removal/correction
20	Deployment	15 - 39	Deployment number
21	ECO-FLNTU S/N	001-9999	Sensor serial number, FLNTU

Table A3. Format of the hourly observational data file for downwelling irradiance (ED) and upwelling radiance (LU).

Column	ID	Value/Range	Comment
1	Year	2005-2019	
2	Month	1-12	
3	Day	0-31	
4	Hour	0-25	
5	Minute	0-60	
6	Second	0-60	
7	Date.Time	732607 - 737335	Matlab format
8-14	Raw Ed(7)	-0.60 25.95	
15	Flag_Offset	0, 1	
16-22	Ed(7)_corr_offset		Corrected for spectral and intersensor offsets
23	Flag_Biofouling	0, 1	Biofouling
24-30	Ed(7)_corr_biofouling	NaN	Values removed
31	Flag_SVO	0, 1	Single value outlier
32	Flag_MDL1	0, 1	< - Method detection level (MDL)
33	Flag_MDL2	0, 1	-MDL to 0
34	Flag_MDL3	0, 1	0 to +MDL
35	Flag Cal	0, 1	Indicates multiplicative scaling
36-42	Ed(7)_final	NaN	Cumulative removal/correction
43	Deployment	15 – 39	Deployment number
44	OCI_507_SN	001-9999	OCI 507 sensor serial number

Table A4. List of submitted data arrays for chlorophyll fluorescence (from FLNTU sensor and each of the three channels of the F3WB sensor), turbidity, spectral irradiance, and central wavelengths of irradiance sensor.

Array Name	**Description**	**Units**	**Array size (row x columns)**	**Format**
H_Chl_2019_v2	hourly chlorophyll fluorescence, FLNTU	mg/m3	9859x23	Table A1
H_NTU_2019_v1	hourly turbidity	NTU	9859x21	Table A2
H_F1_2019_v1	Hourly chlorophyll fluorescence 435 nm excitation, F3WB	mg/m3	9859X23	Table A1
H_F2_2019_v1	Hourly chlorophyll fluorescence 470 nm excitation, F3WB	mg/m3	9859X23	Table A1
H_F3_2019_v1	Hourly chlorophyll fluorescence 532 nm excitation, F3WB	mg/m3	9859X23	Table A1
H_ED_2019_v1	Hourly spectral irradiance, 7 channels	μW/cm2/nm	9859x44	Table A3
H_ED_2018_v3	Hourly spectral irradiance, 7 channels	μW/cm2/nm	18376x44	Table A3
ED7_wave_2019	Irradiance central wavelength	nm	7x1	n/a

Massachusetts Water Resources Authority
100 First Avenue • Boston, MA 02129
www.mwra.com
617-242-6000